

## Synthesis of a Zinc(II) Imidazolium Dicarboxylate Ligand Metal–Organic Framework (MOF): a Potential Precursor to MOF-Tethered N-Heterocyclic Carbene Compounds

Rachel S. Crees,<sup>†</sup> Marcus L. Cole,<sup>‡</sup> Lyall R. Hanton,<sup>§</sup> and Christopher J. Sumbly<sup>\*†</sup>

<sup>†</sup> School of Chemistry & Physics, The University of Adelaide, Adelaide, South Australia 5005, Australia,

<sup>‡</sup> School of Chemistry, University of New South Wales, Sydney, Australia, and <sup>§</sup> Department of Chemistry, University of Otago, Dunedin, New Zealand

Received October 25, 2009

Two new isomeric dinitrile ligands containing imidazolium salt cores have been synthesized from cyanoanilines in good yield. These have been converted to the corresponding dicarboxylic acids using hydrobromic acid, or the dicarboxylic acids were synthesized directly from the analogous cyanoaniline starting material in a two-step, one-pot reaction. The crystal structures of three of the four compounds are reported. Two reaction pathways with metals are possible for the dicarboxylic acids, initially giving rise to metal carboxylate based metal–organic frameworks (MOFs) as described in this work or N-heterocyclic carbene (NHC) metal complexes en route to the synthesis of MOFs containing tethered NHC complexes. The reaction of 1,3-bis(4-carboxyphenyl)imidazolium bromide with zinc nitrate in dimethylformamide (DMF) gave a one-dimensional (1D) MOF containing the intact imidazolium salt. The potentially porous structure, formed from close packing of the 1D necklace-type polymers, contains channels occupied by disordered DMF solvate molecules. A formate anion also bridges the zinc secondary building units in the 1D polymer, which has an undulating structure resulting from the U-shaped conformation of the dicarboxylate imidazolium ligand.

### Introduction

The field of metal–organic framework (MOF) chemistry has been an area of intense study over the past decade.<sup>1–10</sup> The interest in these solid-state materials stems from their applications<sup>11–15</sup> in conductivity, luminescence, magnetism, non-linear optics, chirality, catalysis, and physi- or chemisorption.

The latter two properties are intimately linked with the ability to achieve permanent porosity in a material. In the field of MOF chemistry, work over the last 10–15 years has been focused on the synthesis and study of new MOFs (or coordination polymers). In this regard, new ligands, new ligand and metal combinations, synthetic methods, and structures have been a primary focus, with the ultimate goal of a more rational design approach.<sup>1,2,14</sup> However, in recent years, attention has shifted to investigating and developing the aforementioned properties of known and new MOFs.<sup>14</sup> Recently, during the course of this study, a supramolecular network of a related imidazolium dicarboxylate was reported by Chun et al. with copper(II) that contained a N-heterocyclic carbene (NHC)–copper complex.<sup>16</sup>

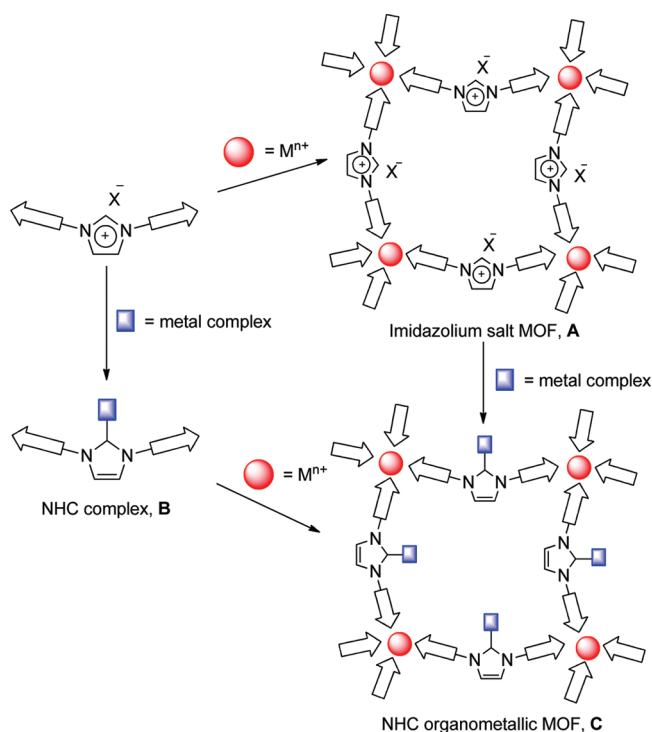
The catalytic activity within a MOF has been investigated for a number of years,<sup>10–13</sup> where these materials are seen as “designable” alternatives to zeolites. A MOF can confer the desirable catalyst properties of size and shape selectivity and ease of recycling. The catalytic activity of a MOF can be derived in a number of ways. First, unsaturated structural metal centers within the MOF can be the active catalysts,<sup>11,12</sup> or the porous MOF itself can act as the catalyst (through the

\*To whom correspondence should be addressed. E-mail: christopher.sumbly@adelaide.edu.au. Phone: +61 8 8303 7406. Fax: +61 8 8303 4358.

- (1) Ferey, G. *Chem. Soc. Rev.* **2008**, 37, 191.
- (2) Yaghi, O. M.; O’Keeffe, M.; Ockwig, N. W.; Chae, H. K.; Eddaoudi, M.; Kim, J. *Nature* **2003**, 423, 705.
- (3) Rosseinsky, M. J. *Microporous Mesoporous Mater.* **2004**, 73, 15.
- (4) Ferey, G.; Mellot-Draznicks, C.; Serre, C.; Millange, F. *Acc. Chem. Res.* **2005**, 38, 217.
- (5) Maspoeh, D.; Ruiz-Molina, D.; Veciana, J. J. *Mater. Chem.* **2004**, 14, 2713.
- (6) Fletcher, A. J.; Thomas, K. M.; Rosseinsky, M. J. *J. Solid State Chem.* **2005**, 178, 2491.
- (7) Kitagawa, S.; Uemura, K. *Chem. Soc. Rev.* **2005**, 34, 109.
- (8) Moulton, B.; Zaworotko, M. J. *Chem. Rev.* **2001**, 101, 1629.
- (9) Zaworotko, M. J. *Chem. Commun.* **2001**, 1.
- (10) Bradshaw, D.; Claridge, J. B.; Cussen, E. J.; Prior, T. J.; Rosseinsky, M. J. *Acc. Chem. Res.* **2005**, 38, 273.
- (11) Janiak, C. *Dalton Trans.* **2003**, 2781.
- (12) Kitagawa, S.; Kitaura, R.; Noro, S. *Angew. Chem., Int. Ed.* **2004**, 43, 2334.
- (13) Tanaka, D.; Kitagawa, S. *Chem. Mater.* **2008**, 20, 922.
- (14) Ferey, G. *Dalton Trans.* **2009**, 4400.
- (15) Farrusseng, D.; Aguado, S.; Pinel, C. *Angew. Chem., Int. Ed.* **2009**, 48, 7502.

- (16) Chun, J.; Jung, I. G.; Kim, H. J.; Park, M.; Lah, M. S.; Son, S. U. *Inorg. Chem.* **2009**, 48, 6353.
- (17) Tanaka, K.; Oda, S.; Shiro, M. *Chem. Commun.* **2008**, 820.

**Scheme 1.** Synthetic Routes to Imidazolium Salt Derived MOFs (A) for Anion or Neutral Small-Molecule Binding, Discrete NHC Complexes (B), and, Ultimately, NHC Organometallic MOFs (C) with Potential Applications as Catalytically Active Materials



incorporation of chiral ligands, for example).<sup>13,17</sup> A third alternative is to generate a MOF that can be used to tether a catalytically active metal complex (in a nonstructural role).<sup>18</sup>

NHCs represent one of the most studied members of the class of compounds referred to as nucleophilic carbenes.<sup>19</sup> NHCs have been known for nearly 50 years,<sup>20</sup> although reports of the first stable NHCs came 30 years later.<sup>21</sup> Since this work was published, NHCs have been reported to be key ligands in a variety of organometallic complexes capable of catalyzing numerous reactions.<sup>22,23</sup> A prominent example is the development of NHC–ruthenium complexes capable of olefin metathesis.<sup>24,25</sup>

As part of our broader research program studying ligands containing electron-deficient [3]radialenes,<sup>26–28</sup> or (thio)amides<sup>29</sup> and (thio)ureas suitable for forming interactions with anions, we have developed the synthesis of cationic imidazolium compounds bearing nitrile, pyridyl, and carboxylate donor groups. When incorporated into MOFs (Scheme 1), these organic groups may generate pockets that are suitable for

binding anionic guests<sup>30,31</sup> or enhancing physisorption of small molecules.<sup>32</sup> In the appropriate frameworks, these will also be available for tethering catalytically active metal complexes by unmasking the imidazolium moiety in a postsynthetic modification.<sup>16</sup>

Recently, Chun et al.<sup>16</sup> reported the synthesis of a closely related imidazolium carboxylate ligand and the concomitant formation of NHC–copper complexes in a MOF. We report our recent work in this area, including the syntheses of four new imidazolium-containing ligands, which, although they do not contain the steric bulk to protect the NHC, are potential precursors to MOF-tethered NHCs. Herein, we demonstrate the differential reactivity of one of the carboxylate derivatives and the synthesis of a new one-dimensional (1D) MOF material with zinc(II) salts.

## Experimental Section

**General Procedures.** Melting points were recorded on an Electrothermal melting point apparatus. IR spectra were collected on a Perkin-Elmer BX FTIR spectrometer as KBr disks. Electrospray (ES) mass spectra were recorded using a Finnigan LCQ mass spectrometer. High-resolution ES mass spectrometry was performed on a Micromass LCT-TOF mass spectrometer at the University of Canterbury. Unless otherwise stated, NMR spectra were recorded on a Varian Gemini 200 or 300 MHz or Varian Unity 600 MHz spectrometer at 20 °C using a 5 mm probe. <sup>1</sup>H NMR spectra recorded in dimethyl sulfoxide (DMSO)-*d*<sub>6</sub>, methanol-*d*<sub>4</sub>, and D<sub>2</sub>O were referenced to the residual solvent peaks 2.50, 3.31, and 4.79 ppm. When required, two-dimensional NOESY, TOCSY, ROESY, and COSY experiments were performed using standard pulse sequences. Unless otherwise stated, the values given for chemical shifts are to the center of a multiplet and multiplicities are listed based on three-bond coupling only. All coupling constants are given in hertz. The Campbell microanalytical laboratory at the University of Otago performed elemental analyses. Unless otherwise stated, reagents were obtained from commercial sources and used as received.

**Ligand Synthesis. 1,3-Bis(4-cyanophenyl)imidazolium Chloride, 3(Cl).** To a stirred solution of paraformaldehyde (0.98 g, 33 mmol) in toluene (50 mL) was added 4-cyanoaniline (**1**; 7.72 g, 65.2 mmol) and aqueous glyoxal [40% (v/v), 4.74 g, 32.6 mmol] followed by the dropwise addition of HCl [37% (v/v), 3.72 mL, 32.6 mmol]. The mixture was refluxed until ca. 6.5 mL of water was recovered via a Dean–Stark apparatus. The solvent was removed in vacuo and the resulting oil triturated with acetonitrile to yield a pale-brown powder (7.50 g, 75%). Conversion to the yellow hexafluorophosphate salt was achieved by stirring the chloride salt in water with excess NH<sub>4</sub>PF<sub>6</sub> and recovering the precipitate by filtration. Mp: 235–236 °C. <sup>1</sup>H NMR (600 MHz, DMSO-*d*<sub>6</sub>): δ 8.13 (d, *J* = 8.4, 4H, H2'/H6'), 8.25 (d, *J* = 8.4, 4H, H3'/H5'), 8.67 (s, 2H, H4/H5), 10.58 (s, 1H, H2). <sup>13</sup>C NMR (600 MHz, DMSO-*d*<sub>6</sub>): δ 113.2, 118.2, 122.4, 123.2, 135.0, 136.4, 138.2. IR (Nujol): ν<sub>max</sub>/cm<sup>-1</sup> 2230 (conjugated CN). ESI-MS: C<sub>17</sub>H<sub>11</sub>N<sub>4</sub> [M<sup>+</sup>] 273 (1%), 272 (16), 271 (83). Anal. Calcd for C<sub>17</sub>H<sub>11</sub>N<sub>4</sub>F<sub>6</sub>P: C, 49.05; H, 2.67; N, 13.46. Found: C, 49.12; H, 2.70; N, 13.52. Crystals of 3(NO<sub>3</sub>) were obtained by the slow evaporation of a 1:1 acetone/acetonitrile solution of 3(PF<sub>6</sub>) and silver(I) nitrate.

**1,3-Bis(3-cyanophenyl)imidazolium Chloride, 4(Cl).** Using the method outlined for the synthesis of 3(Cl), imidazolium salt 4(Cl) was obtained as an off-white powder following trituration

(18) Lassalle-Kaiser, B.; Guillot, R.; Aukauloo, A. *Tetrahedron Lett.* **2007**, *48*, 7004.

(19) Bourissou, D.; Guerret, O.; Gabbai, F. P.; Bertrand, G. *Chem. Rev.* **2000**, *100*, 39.

(20) Wanzlick, H. W.; Schikora, E. *Angew. Chem.* **1960**, *72*, 494.

(21) Arduengo, A. J., III; Harlow, R. L.; Kline, M. *J. Am. Chem. Soc.* **1991**, *114*, 7034.

(22) Herrmann, W. A. *Angew. Chem., Int. Ed.* **2002**, *41*, 1290.

(23) Marion, N.; Nolan, S. P. *Chem. Soc. Rev.* **2008**, *37*, 1776.

(24) Trnka, T. M.; Grubbs, R. H. *Acc. Chem. Res.* **2001**, *34*, 18.

(25) Colacino, E.; Martinez, J.; Lamaty, F. *Coord. Chem. Rev.* **2007**, *251*, 726.

(26) Hollis, C. A.; Hanton, L. R.; Morris, J. C.; Sumby, C. J. *Cryst. Growth Des.* **2009**, *9*, 2911.

(27) Steel, P. J.; Sumby, C. J. *Chem. Commun.* **2002**, 322.

(28) Steel, P. J.; Sumby, C. J. *Inorg. Chem. Commun.* **2002**, *5*, 323.

(29) Sumby, C. J.; Hanton, L. R. *Tetrahedron* **2009**, *65*, 4681.

(30) Custelcean, R.; Moyer, B. A. *Eur. J. Inorg. Chem.* **2007**, 1321.

(31) Custelcean, R. *Chem. Commun.* **2008**, 295.

(32) Higuchi, M.; Tanaka, D.; Horike, S.; Sakamoto, H.; Nakamura, K.; Takashima, Y.; Hijikata, Y.; Yanai, N.; Kim, J.; Kato, K.; Kubota, Y.; Takata, M.; Kitagawa, S. *J. Am. Chem. Soc.* **2009**, *131*, 10336.

**Table 1.** Crystal Data and X-ray Experimental Data for **3**(NO<sub>3</sub>)<sub>2</sub>, **5**(ClO<sub>4</sub>), **6**(FeCl<sub>4</sub>), and **7**

	<b>3</b> (NO <sub>3</sub> ) <sub>2</sub>	<b>5</b> (ClO <sub>4</sub> )	<b>6</b> (FeCl <sub>4</sub> )	<b>7</b>
empirical formula	C <sub>34</sub> H <sub>22</sub> N <sub>10</sub> O <sub>6</sub>	C <sub>17</sub> H <sub>13</sub> ClN <sub>2</sub> O <sub>8</sub>	C <sub>17</sub> H <sub>13</sub> Cl <sub>4</sub> FeN <sub>2</sub> O <sub>4</sub>	C <sub>19.75</sub> H <sub>16.75</sub> N <sub>3.25</sub> O <sub>7.25</sub> Zn
fw	666.62	408.74	506.94	480.98
cryst syst	triclinic	monoclinic	orthorhombic	monoclinic
space group	<i>P</i> $\bar{1}$	<i>P</i> 2 <sub>1</sub> / <i>c</i>	<i>Pnma</i>	<i>C</i> 2/ <i>m</i>
unit cell dimens				
<i>a</i> (Å)	9.0944(9)	9.5620(19)	14.693(3)	20.796(4)
<i>b</i> (Å)	12.7988(13)	10.638(2)	19.809(4)	18.019(4)
<i>c</i> (Å)	14.6289(14)	17.505(5)	7.3570(15)	10.943(2)
$\alpha$ (deg)	109.386(6)			
$\beta$ (deg)	100.961(6)	111.00(3)		91.907(8)
$\gamma$ (deg)	97.844(6)			
<i>V</i> (Å <sup>3</sup> )	1539.9(3)	1662.3(7)	2141.3(8)	4098.3(14)
<i>Z</i>	2	4	4	8
density (calcd) (Mg/m <sup>3</sup> )	1.438	1.633	1.573	1.559
abs coeff (mm <sup>-1</sup> )	0.103	0.284	1.228	1.249
<i>F</i> (000)	688	840	1020	1968
cryst size (mm)	0.42/0.34/0.12	0.19/0.17/0.07	0.17/0.10/0.08	0.26/0.24/0.15
$\theta_{\max}$ of data collection (deg)	27.74	27.07	24.99	27.00
reflns collected	33 987	22 462	24 590	35 436
indep reflns [ <i>R</i> <sub>int</sub> ]	7013 [0.1084]	3575 [0.1020]	1857 [0.1085]	4612 [0.0538]
obsd reflns [ <i>I</i> > 2 $\sigma$ ( <i>I</i> )]	5178	3377	1792	4150
data/restraints/param	7013/0/451	3575/0/253	1857/0/133	4612/2/300
GOF on <i>F</i> <sup>2</sup>	0.996	1.039	1.094	1.078
<i>R</i> 1 [ <i>I</i> > 2 $\sigma$ ( <i>I</i> )]	0.0472	0.0592	0.0964	0.0393
w <i>R</i> 2 (all data)	0.1267	0.1593	0.2249	0.1172

from acetonitrile (7.50 g, 75%). Mp: 220 °C (dec). <sup>1</sup>H NMR (600 MHz, CD<sub>3</sub>OD):  $\delta$  7.90 (t, *J* = 7.8, 2H, H5'), 8.04 (d, *J* = 7.2, 2H, H4'), 8.20 (d, *J* = 7.8, 2H, H6'), 8.34 (s, 2H, H2'), 8.43 (s, 2H, H4/H5), 10.51 (s, 1H, H2). <sup>13</sup>C NMR (600 MHz, CD<sub>3</sub>OD):  $\delta$  116.2, 118.6, 124.4, 127.9, 128.7, 133.4, 135.8, 137.9, one signal overlapped. IR (Nujol):  $\nu_{\max}/\text{cm}^{-1}$  2234 (conjugated CN). ESI-MS: C<sub>17</sub>H<sub>11</sub>N<sub>4</sub> [M<sup>+</sup>] 273 (4%), 272 (18), 271 (78). Anal. Calcd for C<sub>17</sub>H<sub>11</sub>N<sub>4</sub>Cl·<sup>1</sup>/<sub>4</sub>H<sub>2</sub>O: C, 65.69; H, 3.73; N, 18.00. Found: C, 65.23; H, 3.74; N, 18.05.

**1,3-Bis(4-carboxyphenyl)imidazolium Bromide, 5(Br).** To a solution of paraformaldehyde (0.98 g, 33 mmol) in toluene (40 mL) was added 4-cyanoaniline (7.72 g, 65.2 mmol) and aqueous glyoxal [40% (v/v), 4.74 g, 32.6 mmol] followed by the dropwise addition of HCl [37% (v/v), 3.72 mL, 32.6 mmol]. The mixture was refluxed until ca. 6.5 mL of water was recovered using a Dean–Stark apparatus. The solvent was removed in vacuo, HBr (90 mL) added, and the solution heated at reflux overnight. The product was collected as a pale-brown powder by filtration, washed with ethyl acetate, and dried (8.60 g, 69%). Mp: > 300 °C. <sup>1</sup>H NMR (200 MHz, CD<sub>3</sub>OD):  $\delta$  7.88 (d, *J* = 8.4, 4H, H3'/H5'), 8.03 (d, *J* = 8.4, 4H, H2'/H6'), 8.48 (s, 2H, H4/H5), 10.38 (s, 1H, H2). <sup>1</sup>H NMR (200 MHz, DMSO-*d*<sub>6</sub>):  $\delta$  8.09 (d, *J* = 8.5, 4H, H3'/H5'), 8.24 (d, *J* = 8.5, 4H, H2'/H6'), 8.71 (s, 2H, H4/H5), 10.60 (s, 1H, H2), 13.31 (s, b, COOH). <sup>13</sup>C NMR [600 MHz, D<sub>2</sub>O with K<sub>2</sub>CO<sub>3</sub> added to dissolve **5**(Br)]:  $\delta$  121.0, 122.1, 130.4, 130.6, 135.7, 138.1, 173.3. IR (Nujol):  $\nu_{\max}/\text{cm}^{-1}$  1715 (C=O). HRMS. Calcd for C<sub>17</sub>H<sub>13</sub>N<sub>2</sub>O<sub>4</sub> [M<sup>+</sup>]: 309.0875. Found: 309.0862. Anal. Calcd for C<sub>17</sub>H<sub>13</sub>N<sub>2</sub>O<sub>4</sub>Br: C, 52.46; H, 3.37; N, 7.20. Found: C, 52.64; H, 3.54; N, 8.27 (analysis for nitrogen consistently high). Crystals of **5**(ClO<sub>4</sub>) were obtained by the slow evaporation of a methanol solution of **5**(Br) and zinc(II) perchlorate.

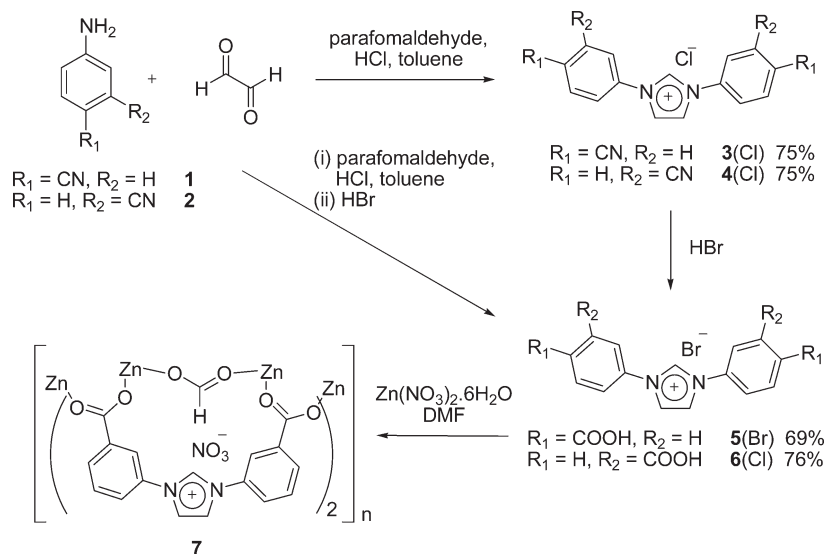
**1,3-Bis(3-carboxyphenyl)imidazolium Chloride, 6(Cl).** Using the method described for **5**(Br), compound **6**(Cl) was isolated from the reaction as an off-white powder by filtration, washed with ethyl acetate, and dried (8.28 g, 76%). Mp: > 300 °C. <sup>1</sup>H NMR (600 MHz, CD<sub>3</sub>OD):  $\delta$  7.82 (t, *J* = 7.8, 2H, H5'), 8.10 (d, *J* = 7.8, 2H, H6'), 8.27 (d, *J* = 7.8, 2H, H4'), 8.38 (s, 2H, H4/H5), 8.48 (s, 2H, H2'), 10.26 (s, 1H, H2). <sup>1</sup>H NMR [600 MHz, DMSO-*d*<sub>6</sub>, with K<sub>2</sub>CO<sub>3</sub> added to dissolve **6**(Cl)]: 7.84 (t, *J* = 7.8, 2H, H5'), 8.15 (m, 4H, H4', H6'), 8.48 (s, 2H, H2'), 8.66 (s, 2H, H4/H5), 10.54 (s, 1H, H2). <sup>13</sup>C NMR (600 MHz, CD<sub>3</sub>OD):  $\delta$  124.4, 125.3, 128.4, 132.4, 133.0, 135.1, 137.0, 137.0, 168.2.

<sup>13</sup>C NMR [600 MHz, DMSO-*d*<sub>6</sub>, with K<sub>2</sub>CO<sub>3</sub> added to dissolve **6**(Cl)]:  $\delta$  122.1, 123.0, 126.4, 130.55, 130.6, 132.9, 135.0, 135.6, 166.1. IR (Nujol):  $\nu_{\max}/\text{cm}^{-1}$  1693 (C=O). HRMS. Calcd for C<sub>17</sub>H<sub>13</sub>N<sub>2</sub>O<sub>4</sub> [M<sup>+</sup>]: 309.0875. Found: 309.0869. Anal. Calcd for C<sub>17</sub>H<sub>13</sub>N<sub>2</sub>O<sub>4</sub>Cl: C, 59.22; H, 3.81; N, 8.13. Found: C, 60.70; H, 3.66; N, 8.10 (analysis for carbon consistently high). Crystals of **6**(FeCl<sub>4</sub>) were obtained by the slow evaporation of a methanol solution of **6**(Cl) and ferric chloride.

**{[Zn<sub>2</sub>( $\mu$ -2-HCOO)(**6**)<sub>2</sub>](NO<sub>3</sub>)·1.5DMF}<sub>n</sub>, **7**.** Ligand **6**(Cl) (50.0 mg, 0.15 mmol) and zinc nitrate (60 mg, 0.30 mmol) were sealed in a 20 mL glass vial with a Teflon-lined screw cap along with dimethylformamide (DMF; 2 mL). The mixture was sonicated for 5 min and then heated at 120 °C for 5 days, cooled, and allowed to stand at room temperature for 7 days. The mother liquor was decanted and the solid washed with DMF and then CHCl<sub>3</sub> to yield **7** as pale-brown powder. Yield: 50.0 mg (69%). IR (KBr disk):  $\nu_{\max}/\text{cm}^{-1}$  1581 (s), 1381 (s). Anal. Calcd for Zn<sub>2</sub>C<sub>40.5</sub>H<sub>38.5</sub>N<sub>6.5</sub>O<sub>14.5</sub>Cl<sub>3</sub> (CHCl<sub>3</sub> solvate): C, 44.81; H, 3.58; N, 8.39. Found: C, 44.96; H, 3.55; N, 8.40. Crystals suitable for X-ray crystallography were obtained by performing the same reaction with a 16-fold excess of zinc nitrate at 100 °C.

**Single-Crystal X-ray Crystallography.** Crystals were mounted under oil on a plastic loop. X-ray diffraction data were collected with (i) Mo K $\alpha$  radiation ( $\lambda$  = 0.710 73 Å) at 90(2) K using a Bruker AXS Single Crystal Diffraction System fitted with an Apex II CCD detector (**3**(NO<sub>3</sub>)<sub>2</sub> and **7**) or (ii) synchrotron radiation ( $\lambda$  = 0.7107 Å) at 150(2) K using the Protein Microcrystal and Small Molecule X-ray Diffraction beamline (PX2) at the Australian Synchrotron (Table 1). Data sets were corrected for absorption using a multiscan method, and structures were solved by direct methods using *SHELXS-97*<sup>33</sup> and refined by full-matrix least squares on *F*<sup>2</sup> by *SHELXL-97*,<sup>34</sup> interfaced through the program *X-Seed*.<sup>35</sup> In general, all non-hydrogen atoms were refined anisotropically, and hydrogen atoms were included as invariants at geometrically estimated positions, unless specified otherwise in additional details below. Figures were produced using the program *POV-Ray*.<sup>36</sup>

(33) Sheldrick, G. M. *Acta Crystallogr.* **1990**, *A46*, 467.(34) Sheldrick, G. M. *SHELXL-97*; University of Göttingen: Göttingen, Germany, 1997.(35) Barbour, L. J. *J. Supramol. Chem.* **2001**, *1*, 189.(36) *POV-Ray 3.6*; Persistence of Vision Raytracer Pty Ltd.: Williamstown, Australia, 2004.

**Scheme 2.** Preparation of Imidazolium Ligands **3**(Cl), **4**(Cl), **5**(Br), and **6**(Cl)

interfaced through the program *X-Seed*. Publication materials were prepared using the program *enCIFer*.<sup>37</sup> Details of data collections and structure refinements are given below. CCDC-752222–CCDC-752225 contain the supplementary crystallographic data for this structure (see the Supporting Information). These data can be obtained free of charge from The Cambridge Crystallographic Data Center via [www.ccdc.cam.ac.uk/data\\_request/cif](http://www.ccdc.cam.ac.uk/data_request/cif).

The structure of compound **7** possesses large voids containing a considerable number of diffuse electron density peaks that could not be adequately modeled as a solvent. The *SQUEEZE* routine of *PLATON*<sup>38</sup> was applied to the collected data, which resulted in reductions in R1 and particularly wR2. R1, wR2, and GOF before the *SQUEEZE* routine: 5.19%, 17.35%, and 1.076. R1, wR2, and GOF after the *SQUEEZE* routine: 3.93%, 11.72%, and 1.078.

**Powder X-ray Diffraction (PX) Analysis.** PXD data were collected using an image-plate Guinier camera set using Co K $\alpha$  radiation at the South Australian Museum. Diffraction data were collected in the range  $2\theta = 5\text{--}100^\circ$  with a step size of  $2\theta = 0.005^\circ$  at 298 K. Theoretical powder patterns were calculated with *MERCURY*<sup>39</sup> using the single-crystal diffraction data generated for **7** as a model.

## Results and Discussion

Two general routes are available for the synthesis of the diarylimidazolium precursors used for the generation of NHCs. The first and less widely utilized route involves appending the appropriate heteroaryl substituents to either imidazole or *N*-methylimidazole,<sup>40</sup> while the second, more common approach, requires formation of the central heterocyclic imidazole ring during the synthesis of the imidazolium compound.<sup>41,42</sup> This second approach requires the synthesis of a diazabutadiene (DAB) intermediate from 2 equiv of an

aniline and an  $\alpha$ -dicarbonyl such as glyoxal, before cyclization of DAB with formaldehyde. In the synthesis of the imidazolium compounds reported here, we opted for the latter method, Scheme 2. Thus, the reaction of the isomeric cyanoanilines (**1** and **2**) with glyoxal and paraformaldehyde yielded **3** and **4** in good yield (75%) for both compounds. These could be isolated as either their chloride (as synthesized, **3**, and **4**) or hexafluorophosphate salts. Conversion to the dicarboxylic acid derivatives **5** and **6** was achieved by treatment of dinitriles **3** and **4** with hydrobromic acid. Other acids such as sulfuric acid were ineffective in this conversion. The synthesis of **5** and **6** could also be carried out in excellent yield in a one-pot, two-stage reaction without isolating the dinitrile compounds. A closely related imidazolium dicarboxylate ligand was recently synthesized from 1,3-bis(4-iodophenyl)imidazolium chloride by a palladium-catalyzed reaction with carbon monoxide in methanol.<sup>16</sup>

Compounds **3–6** were characterized by a combination of NMR and IR spectroscopy, ES mass spectrometry, elemental analysis, and, in the case of **3**(NO<sub>3</sub>), **5**(ClO<sub>4</sub>), and **6**(FeCl<sub>4</sub>), X-ray crystallography. Compounds **3–6** are reasonably soluble in polar solvents, methanol, DMSO, and DMF, and can be made more soluble in chlorinated organic solvents by conversion to their hexafluorophosphate salts. The <sup>1</sup>H NMR spectra of **3–6** all have diagnostic peaks corresponding to the imidazolium H2 proton in the range 10.20–10.60 ppm. IR spectra have characteristic peaks for the C $\equiv$ N stretch at 2230 and 2234 cm<sup>-1</sup> for **3** and **4**, respectively. After conversion to the dicarboxylic acid derivatives **5** and **6**, the C $\equiv$ N stretch disappears and a C=O stretch is observed for both compounds. Elemental analysis for **3** and **4** was readily fitted to the calculated values, but despite consistent analyses, good fits between the calculated and experimental values were not obtained for **5** and **6**. The analyses obtained are consistently high in nitrogen for **5** and high in carbon for **6** presumably because of contamination with residual cyanoaniline [**5**(Br)] starting material or carboxylate [**6**(Cl)] coproduct.

As part of an investigation of the coordination chemistry of **3**, crystals of the compound as its nitrate salt, {**3**(NO<sub>3</sub>)<sub>2</sub>}, were obtained by the reaction of **3**(Cl) with silver(I) nitrate. The asymmetric unit contains two molecules of the cation **3**

(37) *enCIFer*; Cambridge Structural Database Centre: Cambridge, U.K., 2005.

(38) Spek, A. L. *Acta Crystallogr.* **1990**, *A46*, C34.

(39) Macrae, C. F.; Bruno, I. J.; Chisholm, J. A.; Edgington, P. R.; McCabe, P.; Pidcock, E.; Rodriguez-Monge, L.; Taylor, R.; Streek, J. v. d.; Wood, P. A. *J. Appl. Chem.* **2008**, *41*, 466.

(40) Catalano, V. J.; Malwitz, M. A.; Etogo, A. O. *Inorg. Chem.* **2004**, *43*, 5714.

(41) Jung, I. G.; Seo, J.; Chung, Y. K.; Shin, D. M.; Chun, S.-H.; Son, S. U. *J. Polym. Sci., Part A: Polym. Chem.* **2007**, *45*, 3042.

(42) Alexander, S. G.; Cole, M. L.; Morris, J. C. *New J. Chem.* **2009**, *33*, 720.

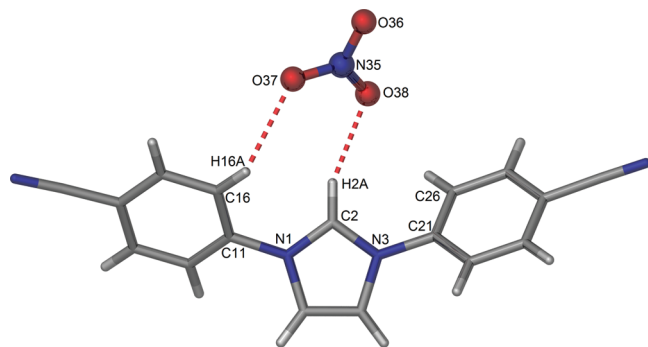


**Figure 1.** Perspective view of one of the molecules of **3** from the crystal structure  $\{3(\text{NO}_3)_2\}$ , confirming the structure of the compound and its rigid angular structure.

and two nitrate counterions. Aside from subtle differences in hydrogen-bonding interactions, both molecules of **3** in the asymmetric unit have near-identical bond lengths and angles. Consequently, the remainder of the discussion focuses on only one of the molecules in the asymmetric unit. The crystal structure confirms the structure of the dinitrile compound **3** (Figure 1) and demonstrates the suitability of these types of compounds as rigid components for MOF synthesis. Ligands constructed on the imidazolium scaffold with donor groups in the 4 position of the phenyl ring attached to the central imidazole (i.e., **3** and **5**) are angular components with approximately  $140^\circ$  between the two donors. In the case of compound **3**, the angle between the two nitrile donors, which are separated by approximately  $14.99 \text{ \AA}$ , is  $143.1^\circ$ .

Compound **3** is not planar in the solid state with torsion angles  $\text{C16-C11-N1-C2}$  and  $\text{C2-N3-C21-C26}$  of  $39.0$  and  $47.2^\circ$ , respectively. In the solid state, **3** and the nitrate anion form an intricate hydrogen-bonded network. Figure 1 illustrates  $\text{C-H}\cdots\text{O}$  hydrogen bonds involving only the nitrate ion that sits in the cleft formed by the imidazolium ring of **3**. The  $\text{C-H}\cdots\text{O}$  hydrogen-bond distances are  $d_{\text{H16A-O37}} = 2.47$ ,  $D_{\text{C16-O37}} = 3.22 \text{ \AA}$  and  $d_{\text{H2A-O38}} = 2.28$ ,  $D_{\text{C2-O38}} = 3.17 \text{ \AA}$ .

Crystals of the two carboxylic acid derivatives **5** and **6** were obtained from attempted reactions of these compounds with transition-metal salts under ambient conditions in methanol. Compound **5** crystallized as a perchlorate salt, **5(ClO<sub>4</sub>)**, following reaction with zinc perchlorate, while **6(FeCl<sub>4</sub>)** crystals were obtained by the cocrystallization of compound **6** and ferric chloride. These structures support spectroscopic data obtained for **5(Br)** and **6(Cl)** and confirm the expected structures for these compounds.

The salt **5(ClO<sub>4</sub>)** crystallized in the monoclinic space group  $P2_1/c$  with one complete molecule of **5** and a perchlorate anion in the asymmetric unit. A perspective view of **5(ClO<sub>4</sub>)** is shown in Figure 2, with the shortest  $\text{C-H}\cdots\text{O}$  hydrogen bonds shown. As expected, the structure is very similar to the dinitrile ligand **3**, with an almost identical angle of  $143^\circ$  between the two carboxylic acid groups. Like the dinitrile **3**, compound **5** is not planar in the solid state, with torsion angles for the biaryl bonds between the central five-membered imidazolium ring and the peripheral phenyl rings of  $32.1^\circ$  ( $\text{C16-C11-N1-C2}$ ) and  $38.0^\circ$  ( $\text{C2-N3-C21-C26}$ ). Once again the anion lies in a central pocket formed by the imidazolium salt, although it is not hydrogen-bonded to H2. The shortest  $\text{C-H}\cdots\text{O}$  hydrogen bonds within this pocket involve H16 and H26, where  $d_{\text{H16-O33}} = 2.60$ ,

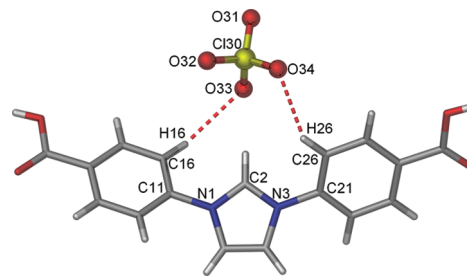


**Figure 2.** Perspective view of **5(ClO<sub>4</sub>)**, confirming the structure of the dicarboxylic acid and its rigid angular structure.

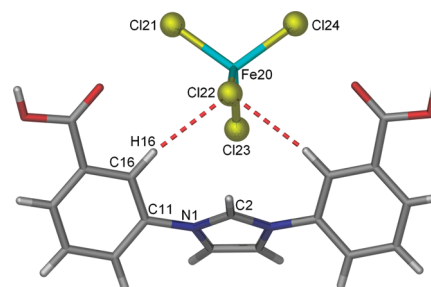


**Figure 3.** Perspective view of **6(FeCl<sub>4</sub>)**, confirming the structure of the dicarboxylic acid **6** and its U-shaped conformation.

$D_{\text{C16-O33}} = 3.26 \text{ \AA}$  and  $d_{\text{H26-O34}} = 2.62$ ,  $D_{\text{C26-O34}} = 3.51 \text{ \AA}$ . The carboxylic acid moieties are also hydrogen-bonded, with much shorter hydrogen-bonding distances ( $1.87$  and  $1.94 \text{ \AA}$ ), to additional perchlorate molecules within the crystal lattice. This prevents the formation of hydrogen bonds between molecules of **5** in the solid state.

The salt **6(FeCl<sub>4</sub>)** crystallized in the orthorhombic space group  $Pmna$  with half a molecule of **5** and half a tetrachloroferrate anion in the asymmetric unit. A perspective view of **6(FeCl<sub>4</sub>)** is shown in Figure 3, with only the shortest  $\text{C-H}\cdots\text{O}$  hydrogen bonds involving the anion that interacts with the imidazolium pocket shown. As expected, the structure is once again similar to compounds **3** and **5** but with quite a different orientation of the two carboxylic acid groups; in the solid-state structure of **6(FeCl<sub>4</sub>)**, compound **6** adopts a U-shaped arrangement of the donors. Compound **6** is non-planar in the solid state with a torsion angle for the biaryl bonds between the central five-membered imidazolium ring and the peripheral phenyl rings of  $45.7^\circ$  ( $\text{C16-C11-N1-C2}$ ). The tetrachloroferrate anion, which is formed in the crystallization solution, lies in a central pocket formed by the imidazolium salt and is weakly hydrogen-bonded to H16, where  $d_{\text{H16-Cl22}} = 2.75$ ,  $D_{\text{C16-Cl22}} = 3.68 \text{ \AA}$ . Once again the carboxylic acid moieties are also hydrogen-bonded, this time with additional molecules of **6**, which results in an undulating 1D hydrogen-bonded tape that extends along the  $b$  axis of the unit cell.

Using solvothermal methods, compounds **5** and **6** have been reacted with a number of different zinc salts (e.g.,  $\text{NO}_3^-$  and  $\text{CH}_3\text{COO}^-$ ), in different stoichiometries, using a range of solvents (e.g., methanol, DMF, and diethylformamide) and with a diverse range of coligands. These reactions invariably led to amorphous or microcrystalline powders. When **6(Cl)** was reacted with zinc nitrate in DMF, a reaction product was formed that is composed of colorless blocklike crystals and a pale-brown-yellow powder. The crystals could be separated manually and were found to be suitable for single-crystal

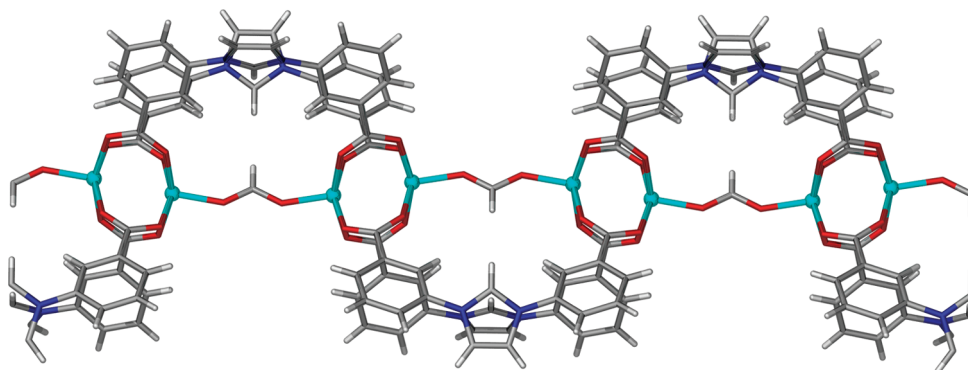


**Figure 4.** Perspective view of the undulating structure of the 1D necklace-type coordination polymer in the crystal structure of **7**.

X-ray crystallography. The structure of **7** was shown to have the formula  $\{[\text{Zn}_2(\mu_2\text{-HCOO})(\mathbf{6})_2](\text{NO}_3) \cdot 1.5\text{DMF}\}_n$ . The phase purity of the bulk samples was confirmed by powder diffraction and IR spectroscopy.

Unfortunately, the structure of **7** was not shown to be the targeted type of three-dimensional MOF but a lower dimensional 1D polymer (Figure 4). Nonetheless, the structure is the first zinc-containing MOF structure incorporating an imidazolium precursor and possesses a number of very interesting features. In particular, it is interesting to note that the imidazolium ring is unaffected by the harsh reaction conditions used during the synthesis of **7**. The 1D polymeric structure is of the necklace type with two molecules of **6** and a formate anion bridging between each dizinc carboxylate secondary building unit (SBU). The cleft formed by the two molecules of **6** houses a nitrate anion and a DMF solvate molecule.

Compound **7** crystallizes in the monoclinic space group  $C2/c$  with a zinc cation, two half-ligand components (both on mirror planes), half a formate anion, half a nitrate anion, and two disordered and partially occupied DMF molecules in the asymmetric unit. The residual electron density was found to be located in channels in the structure but was unable to be accurately modeled. The *SQUEEZE* routine of *PLATON*<sup>38</sup> was applied to the data.

The dizinc carboxylate SBUs are paddlewheel clusters<sup>43</sup> that are commonly observed with carboxylate ligands (Figure 5). The zinc atoms are separated by 3.01 Å with typical Zn–O bonds of between 2.022(2) and 2.062(2) Å. The dizinc SBUs are capped by oxygen atoms from a bridging formate anion with a Zn–O bond length of 1.963(2) Å. Thus, the zinc atoms are five-coordinate with a  $\tau_5$  value of 0,<sup>44</sup> which indicates a square-pyramidal geometry. Within the 1D polymer, each SBU is connected to an adjacent SBU by two molecules of **6** and a  $\mu_2$ -bridging formate anion. Each dizinc SBU is separated from an adjacent SBU by 9.01 Å.

The U-shaped conformation of ligand **6**, observed in the structure of **6**(FeCl<sub>4</sub>), is maintained in the MOF **7**. This results in an undulating or zigzag structure to the 1D polymer. The nitrate anion and a DMF solvate molecule are hydrogen-bonded within the U-shaped clefts of the two molecules of **6** that connect two zinc SBUs. The C–H···O hydrogen-bond distances involving the imidazolium H2 protons and the oxygen atoms of the nitrate anion (O67)

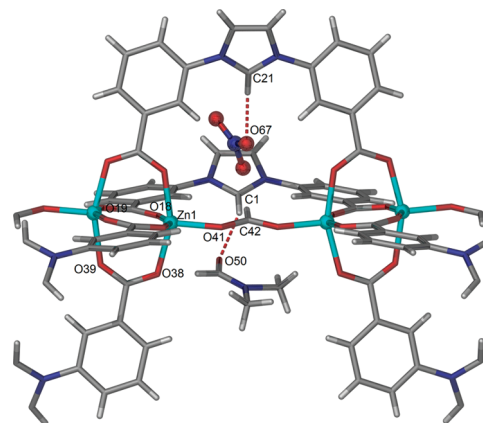


**Figure 5.** Perspective view of the  $\text{Zn}_2$  SBUs in **7**. The  $\mu_2$ -bridging formate anion, a hydrogen-bonded nitrate anion, and a DMF solvate molecule are shown in the pocket formed by two molecules of **6**, which connect the  $\text{Zn}_2$  SBUs in the structure. Selected bond lengths (Å) and angles (deg): Zn1–O41 1.963(2), Zn1–O18 2.022(2), Zn1–O39 2.039(2), Zn1–O19 2.060(2), Zn1–O38 2.062(2); O41–Zn1–O18 109.34(7), O41–Zn1–O39 101.48(7), O18–Zn1–O39 88.38(7), O41–Zn1–O19 92.55(7), O18–Zn1–O19 158.10(8), O39–Zn1–O19 86.64(7), O41–Zn1–O38 100.00(7), O18–Zn1–O38 90.17(7), O39–Zn1–O38 157.69(7), O19–Zn1–O38 86.45(7).

and DMF solvate (O50) are  $d_{\text{H21-O67}} = 2.10$ ,  $D_{\text{C21-O67}} = 3.11$  Å and  $d_{\text{H1-O50}} = 2.31$ ,  $D_{\text{C1-O50}} = 3.19$  Å.

Formate has been previously used for the formation of MOFs.<sup>45</sup> The inclusion of a formate ion in the structure of **7** is serendipitous, although we have also tried introducing other carboxylate ligands into the reaction mixture. It has two probable origins, either from decomposition of the DMF solvent<sup>46</sup> or from decarboxylation of the ligand. With the isomeric carboxylic acid ligand **5**, we have also observed the formation of MOFs containing only formate as a ligand under quite similar conditions. No evidence for the decarboxylation of either **5** or **6** has been observed, and presumably the formate observed in **7** arose from decomposition of the solvent during the reaction.<sup>46</sup>

The 1D necklace-type coordination polymers extend along the *b* axis of the unit cell. The arrangement of the ligands around the polymer leads to a cross-shaped structure (when viewed along the polymer chain) that interdigitates to complete the crystal packing (Figure 6a). The crystal structure of

(43) Vagin, S. I.; Ott, A. K.; Rieger, B. *Chem.-Ing.-Tech.* **2007**, *79*, 767.

(44) Addison, A. W.; Rao, T. N.; Reedijk, J.; Rijn, J. v.; Verschoor, G. C. *J. Chem. Soc., Dalton Trans.* **1984**, 1349.

(45) Wang, Z.; Zhang, Y.; Kurmoo, M.; Liu, T.; Vilminot, S.; Zhao, B.; Gao, S. *Aust. J. Chem.* **2006**, *59*, 617.

(46) Burrows, A. D.; Cassar, K.; Friend, R. M. W.; Mahon, M. F.; Rigby, S. P.; Warren, J. E. *CrystEngComm* **2005**, *7*, 548.

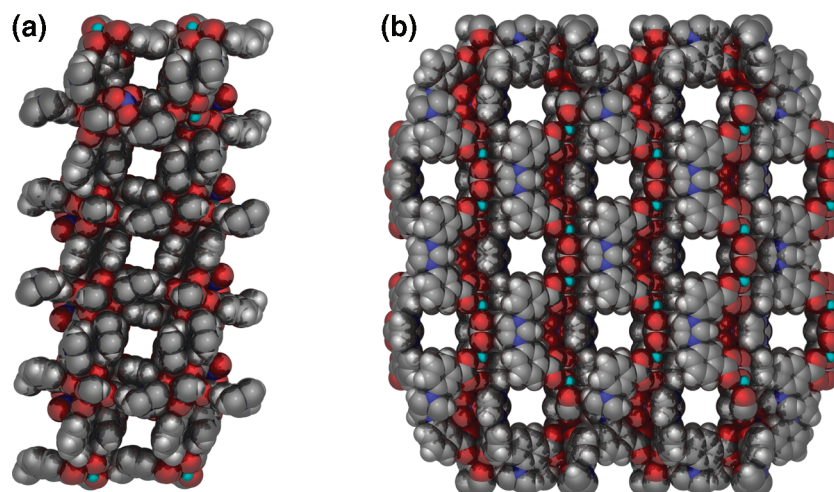


**Figure 6.** Perspective views of a space-filling representation of **7** viewed down (a) the *b* and (b) *c* axes, respectively. Disordered solvent molecules are not shown.

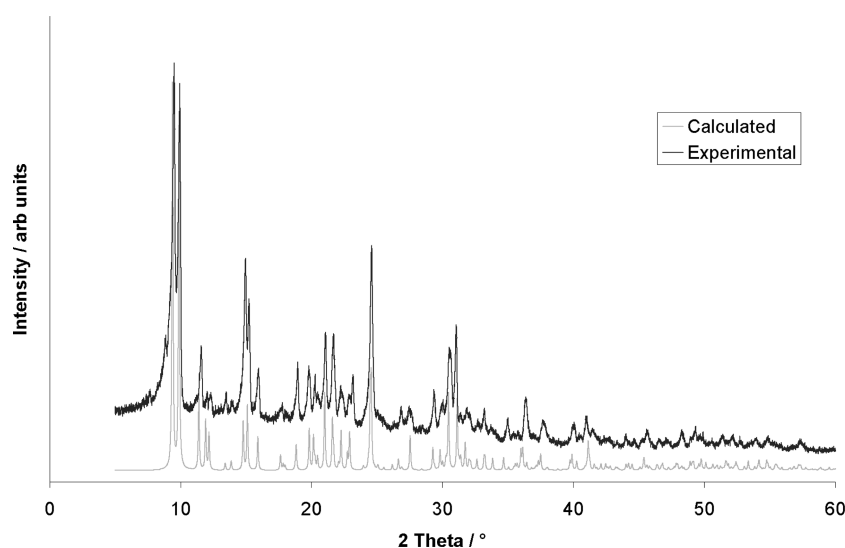


**Figure 7.** Comparison of the experimental PXD data for a sample of as-synthesized **7** and the calculated pattern from single-crystal X-ray data for **7**.

**7** also reveals that the 1D polymers pack in the crystal with weak  $\pi$ -stacking interactions between the chains. The structure has disordered DMF solvate molecules in channels that extend along the *b* and *c* axes (Figure 6b). The channels that are directed along the *c* axis are much larger, and we are in the process of investigating the porosity and sorption characteristics of **7**.

The synthesis of compound **7** has been studied under a number of different reaction conditions. The best yields of **7** as a pure phase were obtained by heating the reaction mixture consisting of **6**(Cl) and zinc nitrate (1:2–1:4 L:M ratios) at 120–130 °C for 4–5 days. In this manner, crystalline powders in up to 69% yield were obtained. At higher temperatures and using higher ratios of zinc nitrate, the isolated material contained very little **7** (although at 120–130 °C crystals suitable for X-ray crystallography were obtained despite a vast excess of zinc nitrate). Reactions undertaken at lower temperatures gave an amorphous material in low yield. PXD studies were undertaken to investigate further the characteristics of **7** and, in particular, to compare the single-crystal structure and the bulk material of **7**. The PXD patterns were recorded

for solvated samples from bulk preparations of **7**. Comparison of the patterns for bulk samples of **7** [prepared from **6**(Cl) at 120 or 130 °C with 2 or 4 equiv of zinc nitrate] and the calculated pattern for **7** (from the single-crystal structure) showed that, with the exception of a few intensity differences, the patterns were in good agreement with each other (Figure 7).

### Conclusion

In this paper, we have described the high-yielding synthesis of four new imidazolium salt ligands **3–6** bearing additional donor groups suitable for the formation of MOFs. These ligands were prepared in one or two simple steps from commercially available anilines. While these ligands do not have the steric bulk around the imidazolium moiety commonly found in such compounds, they are useful and effective structural analogues for more bulky and complicated imidazolium ligands. The crystal structures of compounds **3** and **5** reveal that these compounds are angular components with approximately 143° between the donor groups, while **6** has a U-shaped conformation in the solid state.

When **6**(Cl) was reacted with zinc nitrate, using solvothermal conditions, an unusual dizinc paddlewheel-based MOF was formed. In addition to having an undulating 1D necklace-type structure that incorporates an anionic formate bridging ligand, the 1D polymeric material is packed in the crystals with a potentially porous structure. The imidazolium core is unaffected by the harsh conditions employed in this reaction and is available for subsequent postsynthetic modifications that are a current focus for our research. This result, along with the structures recently reported by Chun et al.,<sup>16</sup> suggests that the future for MOF materials formed from such imidazolium ligands is bright. Our future investigations will focus on the synthesis of further MOF structures derived from imidazolium-containing ligands and, in particular, the study of postsynthetic modifications or the physisorption of gases within MOF **7** and other similar structures.

**Acknowledgment.** C.J.S. thanks the Australian Research Council for an Australian Post-Doctoral

Fellowship and a Future Fellowship (Grant FT099-1910) and for support of this research through a Discovery Project (DP0773011). The University of Otago is acknowledged for providing access to facilities for X-ray crystallography. The Australian Synchrotron is thanked for funding travel and access to the PX1 and PX2 beamlines (AS091 and AS092). The views expressed herein are those of the authors and are not necessarily those of the owner or operator of the Australian Synchrotron. The authors thank Prof. Allan Pring and Dr. Jiafang Bei from the South Australian Museum for recording the PXD data. Dr. Jonathan Morris is acknowledged for helpful discussions.

**Supporting Information Available:** NMR spectra for **5**(Br) and **6**(Cl) and crystallographic information files in CIF format for  $\{\mathbf{3}(\text{NO}_3)\}_2$ , **5**(ClO<sub>4</sub>), **6**(FeCl<sub>4</sub>), and **7**. This material is available free of charge via the Internet at <http://pubs.acs.org>.